PROCEEDINGS, 50th Workshop on Geothermal Reservoir Engineering
Stanford University, Stanford, California, February 10-12, 2025
SGP-TR-229

Forty Years of Production from the Steamboat Geothermal Field: Numerical Model Update

Sulav Dhakal, Drew Spake, Lu Lee, Danny Feucht, John Murphy, John Akerley, Adam Johnson, Ryan Libbey, Paul Spielman

Ormat Technologies, Inc., 6884 Sierra Center Parkway, Reno, NV 89511

sdhakal@ormat.com

Keywords: Steamboat Geothermal Field, Numerical Modeling, Case Study, Nevada, Ormat, Great Basin

ABSTRACT

The Steamboat geothermal field is a Great Basin geothermal system in Reno, Nevada, generating 79 MW net electricity using five zero-greenhouse gas emissions powerplants with full mass reinjection as of 2020. It has been in operation since 1987 and with consolidation of ownership under Ormat since 2004. A numerical reservoir model was developed, calibrated to natural state temperature and pressure conditions, measured production temperatures from 28 wells, the reservoir pressure history, and reservoir tracer tests conducted throughout the operational history.

The numerical model honors the updated geologic and conceptual model for Steamboat, which is characterized by high-angle NE striking faults. These faults control the location of 220-240°C upflow beneath Steamboat Hills and contribute to the 3+ km-long NE-directed outflow to Lower Steamboat. In addition, there is evidence of distributed permeability in the host rock, particularly in Lower Steamboat where unloading features in the granodiorite may be responsible for low-angle faulting and high stratigraphic permeability. Production wells at Steamboat are located in both the upflow and lower temperature outflow of the system. Production temperature decline varies across different parts of the reservoir and is driven by factors such as permeability, and proximity to upflow and reinjection. The highly permeable faults and distributed permeability at Steamboat support high flowrates with low pressure interference and minimal long-term pressure decline.

The large scale, long history and unique structural geometry of Steamboat geothermal reservoir is captured in this study as Ormat continues to optimize its development and operational strategy.

1. INTRODUCTION

1.1 Conceptual Model

The Steamboat geothermal system is a fault-focused Great Basin geothermal system in South Reno/Truckee Meadows between the Carson and Virginia mountain ranges, Nevada. Heat for the system is sourced by fluids circulating along deep-seated fracture networks in a region of thinned lithosphere and corresponding elevated background crustal heat flow (e.g., Wisian et al., 1999; Blackwell, 2013). There is some evidence that a cooling crustal magma body also augments the heat flow for this system; e.g., the occurrence of young (1.1 Ma) rhyolite domes at Steamboat Hills (Upper Steamboat) and by elevated helium isotope ratios (R_a = >6) from fluid samples (Kennedy and Soest, 2007). The presence of a magmatic heat source is consistent with the high natural state system temperatures found at Steamboat, which are above average for deep-circulation geothermal systems across the Basin & Range. Lithosphere degradation and associated asthenospheric upwelling is thought to be a driving force responsible for magma generation elsewhere in the Walker Lane and Eastern California Shear Zone, e.g., Coso and Long Valley (Putirka et al., 2012), and may play a role in magmatism in the crust beneath Steamboat as well.

The geologic conceptual model divides the Steamboat reservoir into three areas within the system: Upper Steamboat, Middle Steamboat, and Lower Steamboat. Upper Steamboat is composed primarily of Triassic-Jurassic metasedimentary and metavolcanic rocks intruded by Jurassic-Cretaceous granitic plutons. These host rocks are deformed by high-angle faults hosting an upflow of 240°C under Upper Steamboat. The faults also control the permeability in Upper Steamboat. The geothermal fluid traverses northeast trending faults and cools as it reaches Middle and Lower Steamboat, reaching a maximum natural state temperature of 184°C and 168°C in Middle and Lower Steamboat respectively. Middle Steamboat is characterized by acid sulfate and argillic alteration at the surface and has extremely high permeability along major faults. This contributes to high productivity/injectivity in wells in the area. Lower Steamboat is notable for the presence of large sinter terraces exposed at surface, while the subsurface is characterized by densely fractured granodiorite host rock with low angle fracturing contributing to high horizontal permeability. Lower Steamboat historically hosted hot springs, mud pots, active sinter deposition and active geysers (White 1967). The system is confined by a low permeability layer of argillic alteration, which acts as a caprock to the system and as a partial control on lateral outflow of the system directed toward Lower Steamboat. The caprock is not a perfect seal, as demonstrated by the occurrence of localized zones of acid-sulfate alteration in Middle/Lower Steamboat, especially near major fault intersections, and robust surface manifestations and sinter deposits in Lower Steamboat. The permeable structures and fluid transport pathways at Steamboat have been identified and confirmed by using geologic mapping, the occurrence of surface manifestations, Formation Microresistivity Imaging (FMI) logs, geophysical surveys, and chemical tracer studies (dePolo, 2017; Feucht et al. 2023; Silberman et al. 1979; Walsh et al., 2010). Figure 1 shows the major faults and the surface location of wells at Steamboat.

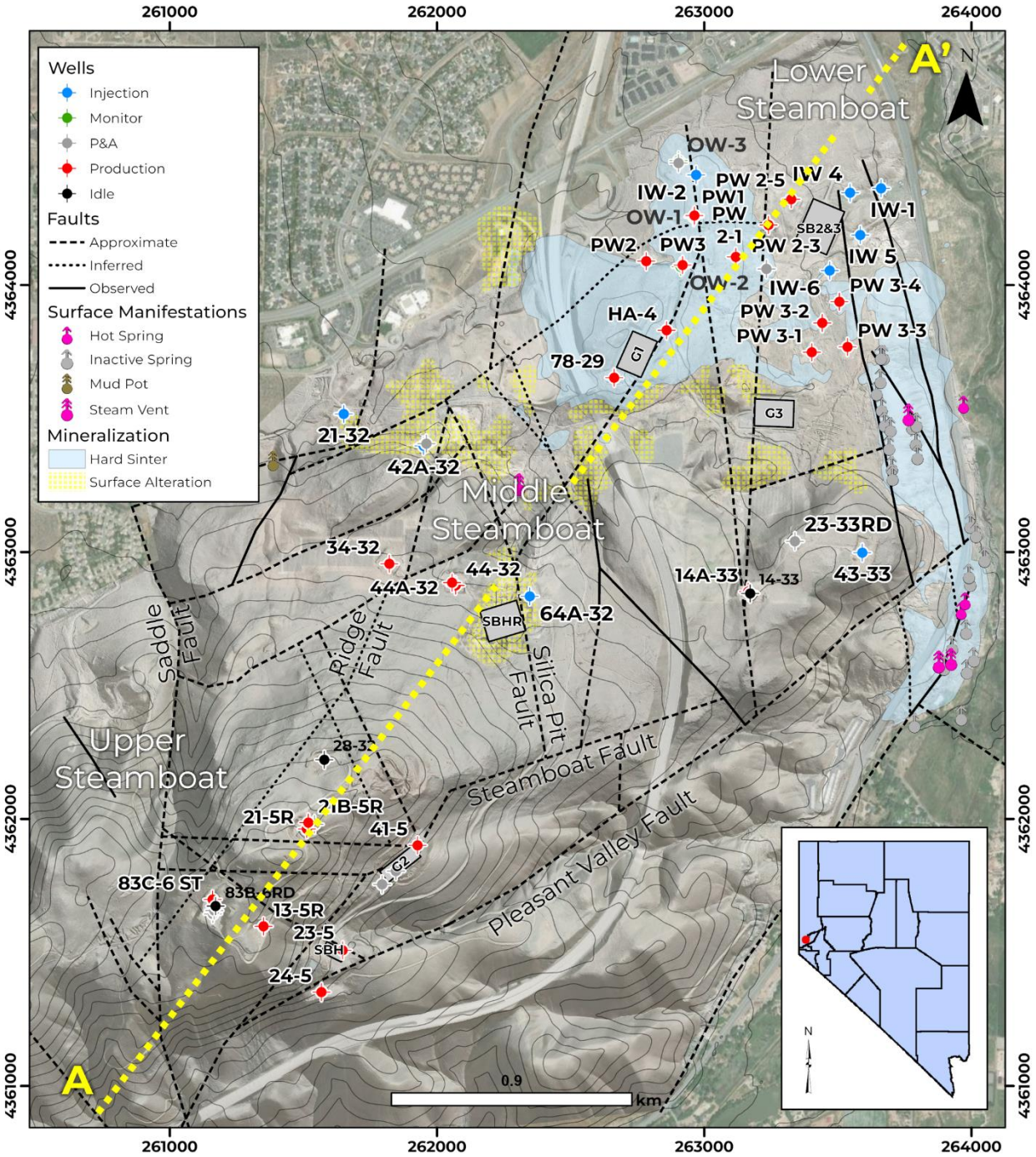

Figure 1: Summary map showing major faults, hydrothermal alteration and surface manifestations, and geothermal development at Steamboat Geothermal Complex.

Feedzones at Steamboat vary in each area of the reservoir. The depth of feedzones in Upper Steamboat are generally 750-1000 m below ground level (BGL; ~1000 mRSL). Feedzone depths are much shallower in Lower Steamboat, averaging 150-300 mBGL (~1200 mRSL). Since production is spread out over both upflow and outflow, there is a wide range of production temperatures in the field, with initial production temperatures exceeding 230°C at Upper Steamboat and 168°C in Lower Steamboat. Despite the very high temperatures in Upper Steamboat, temperature profiles in this region are characterized by broad temperature reversals at the bottoms of wells, suggesting that they are proximal to, but not directly penetrating into upflow. Permeabilities encountered by wells in between to the main NE trending faults and structures observed in image logs have been identified as transverse NW trending faults. Figure 2 shows the conceptual model of Steamboat geothermal field that informs the numerical model.

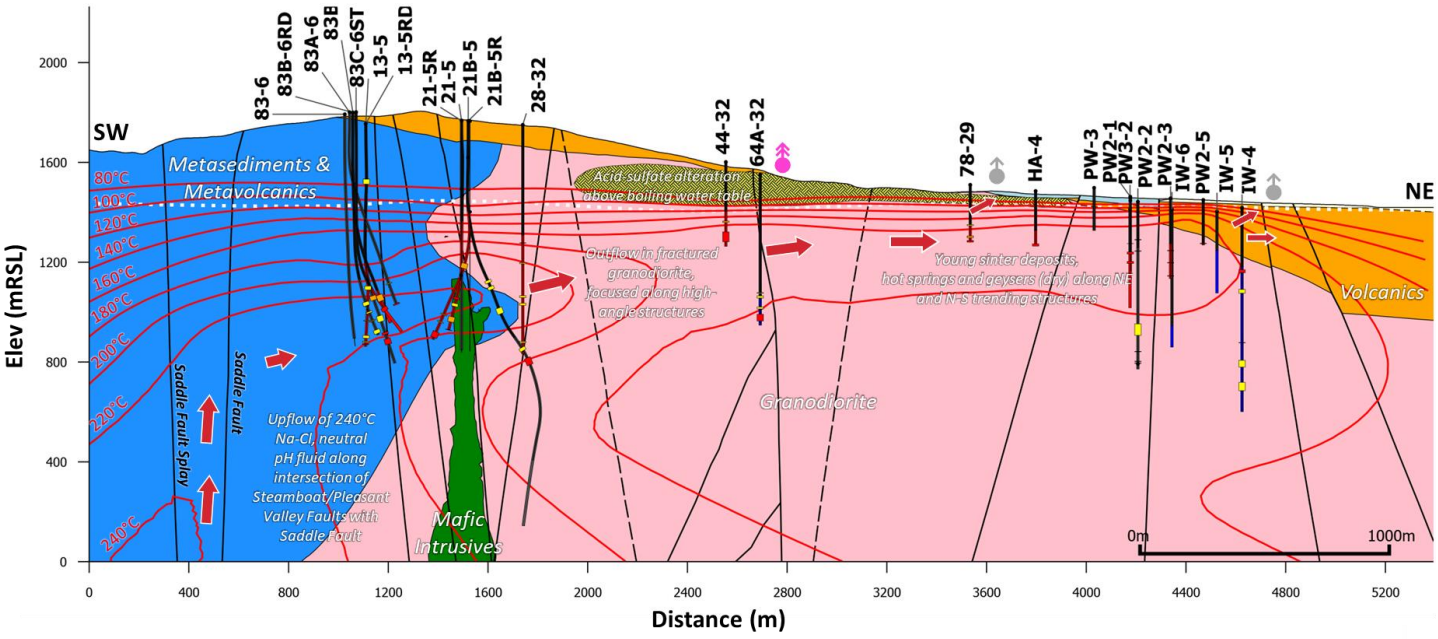

Figure 2: Conceptual model section with lithology, major structures, wells, and natural state isotherms showing upflow at Upper Steamboat and an outflow zone extending to Lower Steamboat.

1.2 Development History

Geothermal development at Steamboat started with direct use in heated baths and pools in the early twentieth century with the first wells drilled in 1920s for constant supply of hot water (Combs and Goranson, 1994). Commercial use of the hot springs for heated baths continues in the area. Exploration and development for electricity generation began in the 1970s with thermal gradient holes and stratigraphic test holes in a partnership of Gulf Oil Company and Phillips Petroleum Company (Combs and Goranson, 1994). Later, Chevron Geothermal Company and Yankee Caithness Joint Venture acquired the project (Goranson, et al., 1990). The first two geothermal plants, Steamboat 1 and Steamboat Hills were commissioned in 1986 under SB Geo Inc. and 1988 under Caithness Power Inc. respectively (Goranson, et al., 1990, Ayling, 2020). Steamboat 2 and Steamboat 3 were commissioned in 1992 at Lower Steamboat. Ormat acquired the four powerplants in 2004 and developed three additional powerplants (Galena 1, 2, 3), decommissioned SB1 and SB Hills, and combined the Steamboat 2 and Steamboat 3 powerplants. Steamboat Hills Repower was commissioned in 2020, taking the generation of the total facility to 79 MW as of 2024. Figure 3 shows the development history of the Steamboat geothermal complex, noting power plant start dates and drilling dates for wells that were used for active production or injection. As of 2024, the power plants are supported by 24 active producers and 9 active injectors. There are over 100 wells in the area including water wells, thermal gradient wells and stratigraphic wells. Production has steadily increased throughout the years as more wells were brought online at Steamboat and as of 2024 almost all production wells are pumped, with only one artesian well remaining (Richardson and Webbison, 2024). Figure 4 shows the total production and injection throughout the history of Steamboat geothermal complex.

The geothermal complex has five powerplants generating 79 MW_{net} of zero greenhouse-gas electricity with an average production of 2940 kg/s in the year 2024 (Figure 5); this is currently the highest mass-flow rate operation of any geothermal power plant complex in the Great Basin. Historically, due to the nature of flash steam powerplants, the Steamboat Hills operations had only about 80-90% reinjection. However, since the acquisition by Ormat and the commission of binary powerplants and retrofitting the existing steam generator with bottoming unit, all produced geothermal fluid is reinjected back into the system.

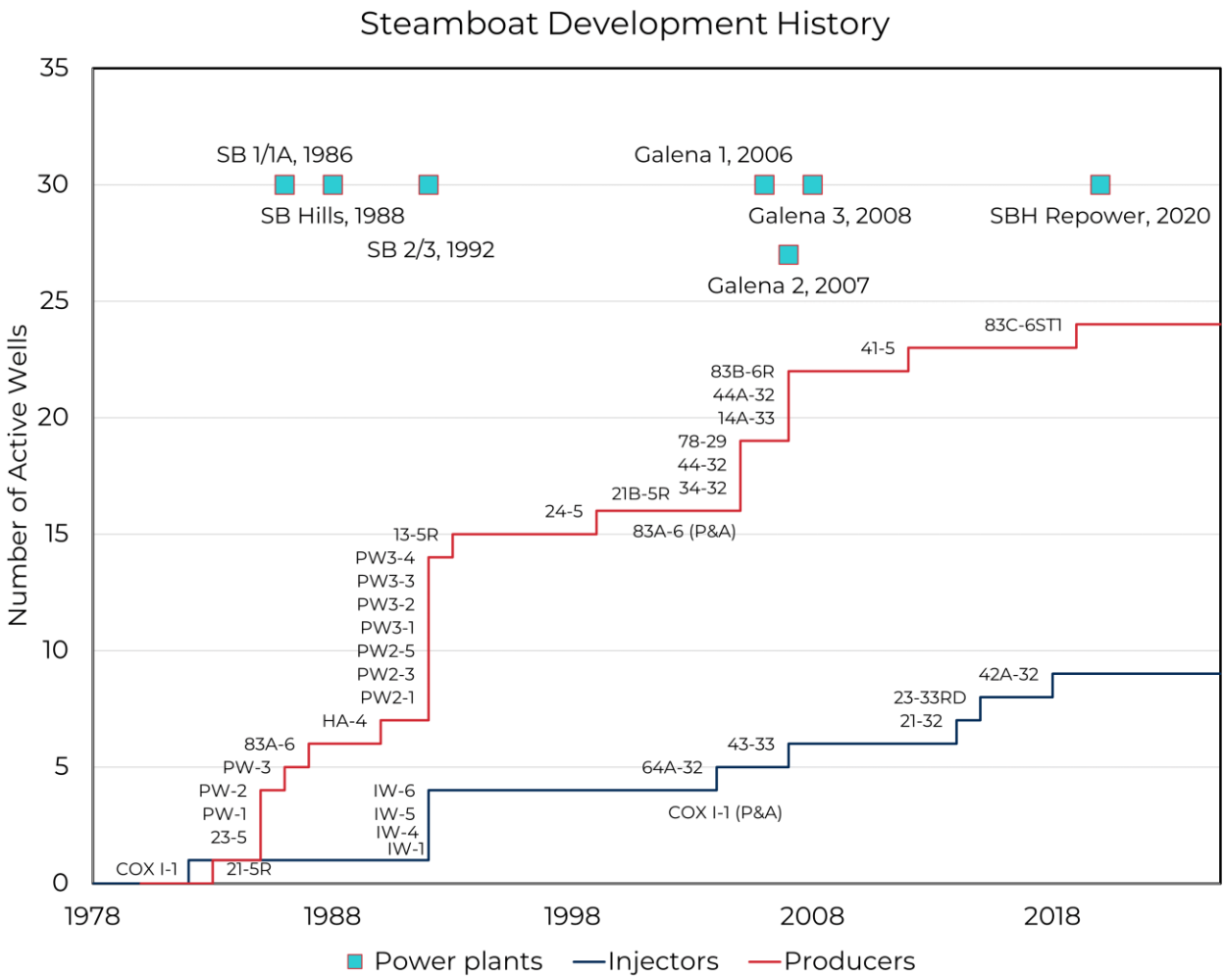

Figure 3: Development history of Steamboat Geothermal Complex.

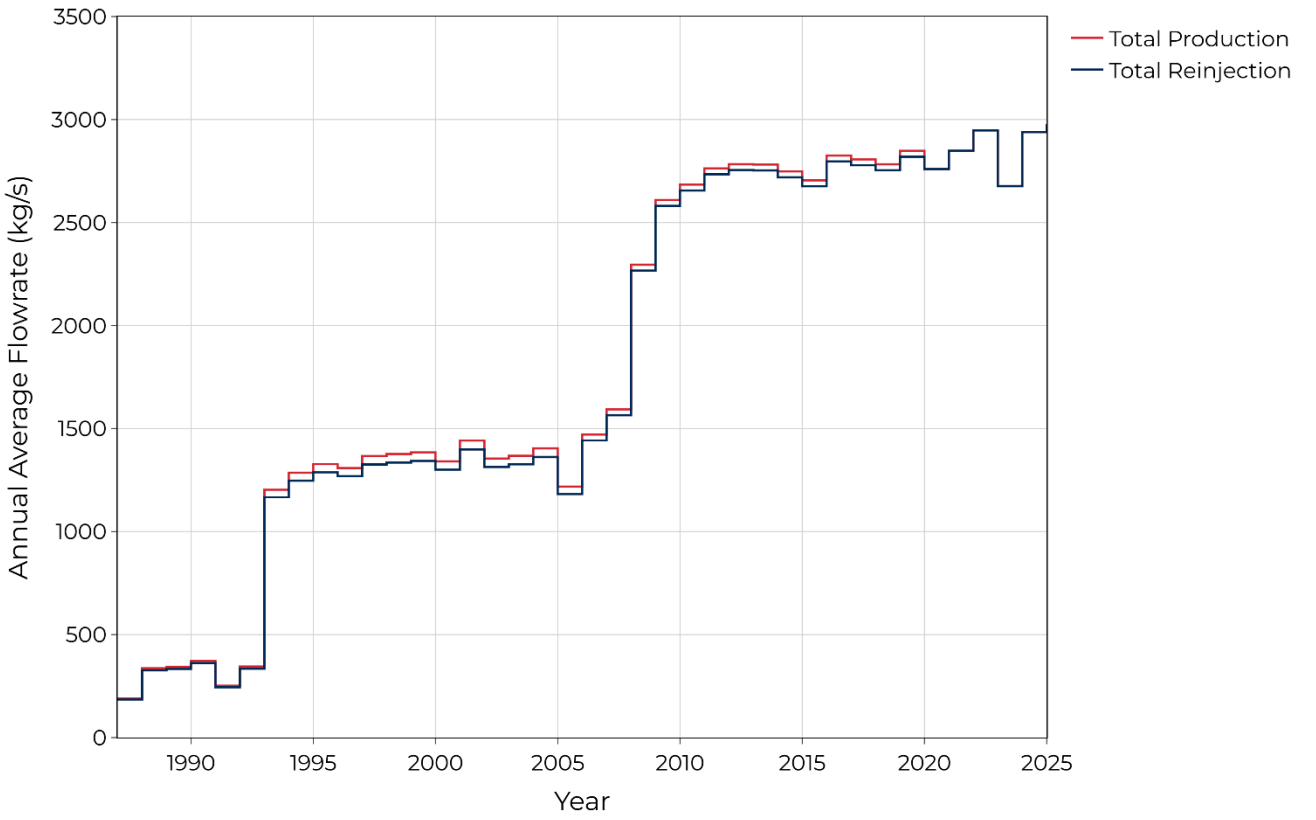

Figure 4: Total annual average production and injection at Steamboat Geothermal Complex.

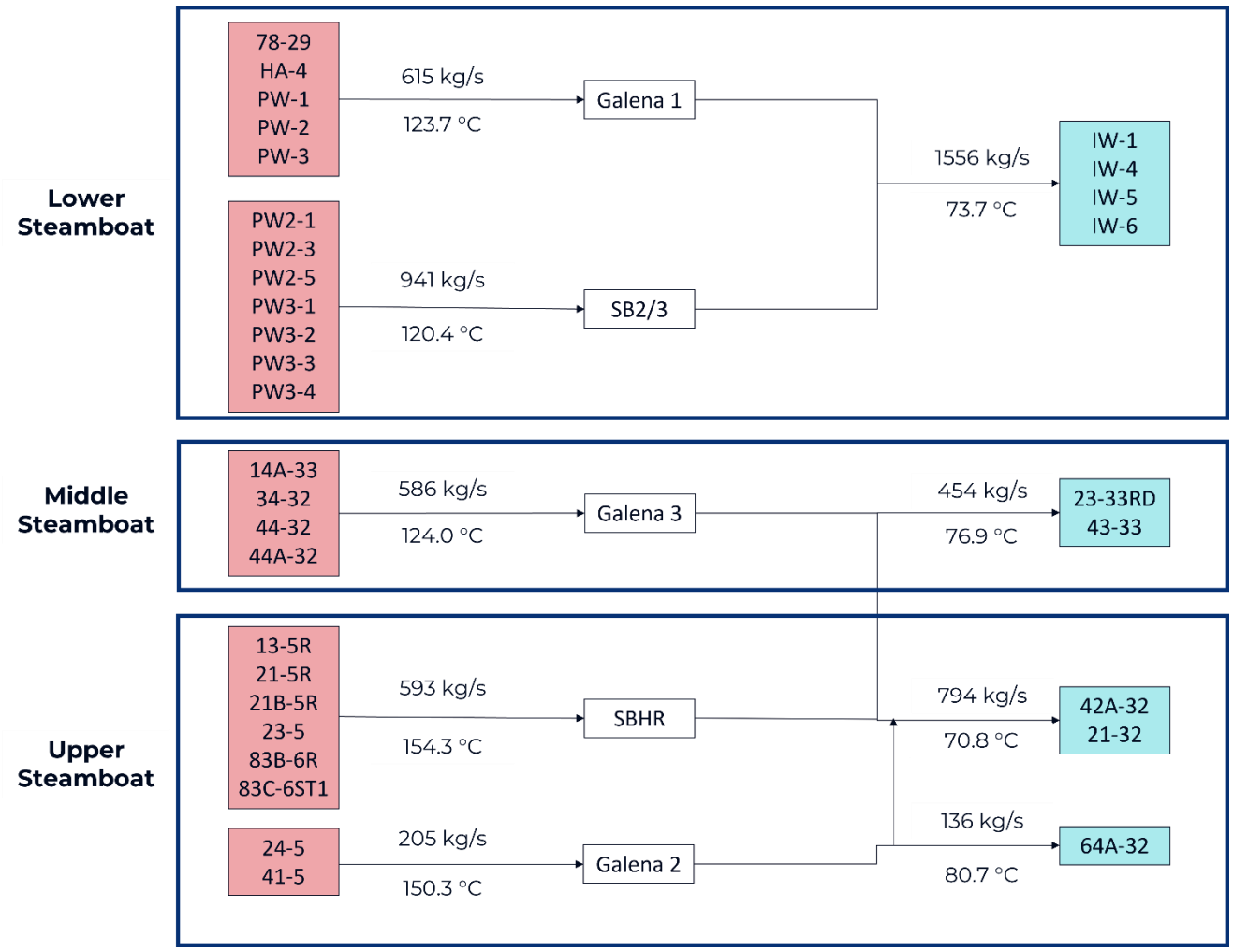

Figure 5: Steamboat geothermal complex configuration with average flow rates and temperatures in 2024.

2. NUMERICAL MODEL

Development and calibration of numerical models for such a complex and diverse geothermal resource is an important aspect of reservoir engineering and has been historically relied upon by the industry for making resource management decisions. Internal numerical models were developed in 1993 and 2002 to reproduce the natural state temperature and early temperature decline. A comprehensive numerical reservoir model was previously developed in a collaborative effort with Ormat and industry experts using historical data and conceptual model (Bjornsson et al., 2014). The model was successful in calibrating the natural history of the geothermal system and calibration of some wellfield data. However, recent developments in computational tools, updates to the conceptual understanding of the system, and the need to develop a consistently up-to-date reservoir model by having it done by an in-house modeling team led to this modeling work. The numerical model was developed in conjunction with the conceptual model in a collaborative effort to reflect the current understanding of the reservoir and wellfield data.

The model was developed in the Volsung reservoir and wellbore modeling software package (Franz and Clearwater, 2021). It uses a finite volume simulator to solve mass and energy balance equations. The numerical model is a 15 km x 15 km single porosity model with 100mx100m grid size and 157388 cells. The reservoir boundary extends from 254000 m to 269000 m East and 4354500 m to 4369500 m North (WGS84 UTM zone 11N). The vertical resolution ranges from 25m to 500 m with elevation ranging from 1750mRSL to -1000mRSL. Single porosity model was used because of high fracture density at Steamboat, high background permeability and validated with temperature decline trends. Inclusion of dual porosity did not improve the calibration and hence it was not used in the model.

The model rock types and permeabilities are populated by using the conceptual model to map faults and volumes onto the reservoir mesh. The model has 3 major SW-NE trending faults transporting hot upflow fluid. These main upflow faults are bridged by subsidiary structures varying in attitude from NNW-SSE, N-S, NE-SW, to E-W. The upflow is towards the southwest direction of the intersection of two major faults. These faults transport hot water from Upper Steamboat towards Lower Steamboat along with north- to NE-trending faults. Upper Steamboat wells have shown conductive temperature regime at shallow depths above about 1000 mRSL to 1200 mRSL. Therefore, fault

depths are adjusted according to the well's natural temperature distribution and a low permeability rock type (Upper Steamboat Shallow) was used above those depths. Permeability anisotropy was assigned throughout the reservoir with 10:1 (kx:kz), except for Lower Steamboat faults where it is 15:1 as we see more horizontal stratigraphy influencing fluid flow and deeper injectors not cooling the shallow producers rapidly even though they are located closely at the surface. All of the parameters are calibrated based on natural temperature and pressure distribution, pressure change, temperature decline, and tracer return. The numerical model has a single component fluid (pure water, IAPWS-IF97). Throughout the simulation, the reservoir has liquid phase as has and is encountered in the field through time.

2.1 Initial and Boundary Conditions

The initial condition of the reservoir is determined by simulating a natural state model based on the boundary conditions determined from the conceptual geological model (Figure 6).

Top Boundary: Top boundary of the reservoir is a fixed boundary with temperature of 12°C and 1 atm pressure. A very low permeable layer (0.001mD) is used at 1400 mRSL to keep the pressure at the atmospheric level and a conductive temperature regime up to the top of the reservoir.

Side Boundary: The side boundaries are no-flow boundaries except for the surface outflow towards the northeastern corner at the top of the reservoir at constant hydrostatic pressure.

Bottom Boundary: The bottom boundary is at a constant temperature of 210°C with constant mass upflow through the upflow zone below Upper Steamboat at 240°C at 70 kg/s total flow rate.

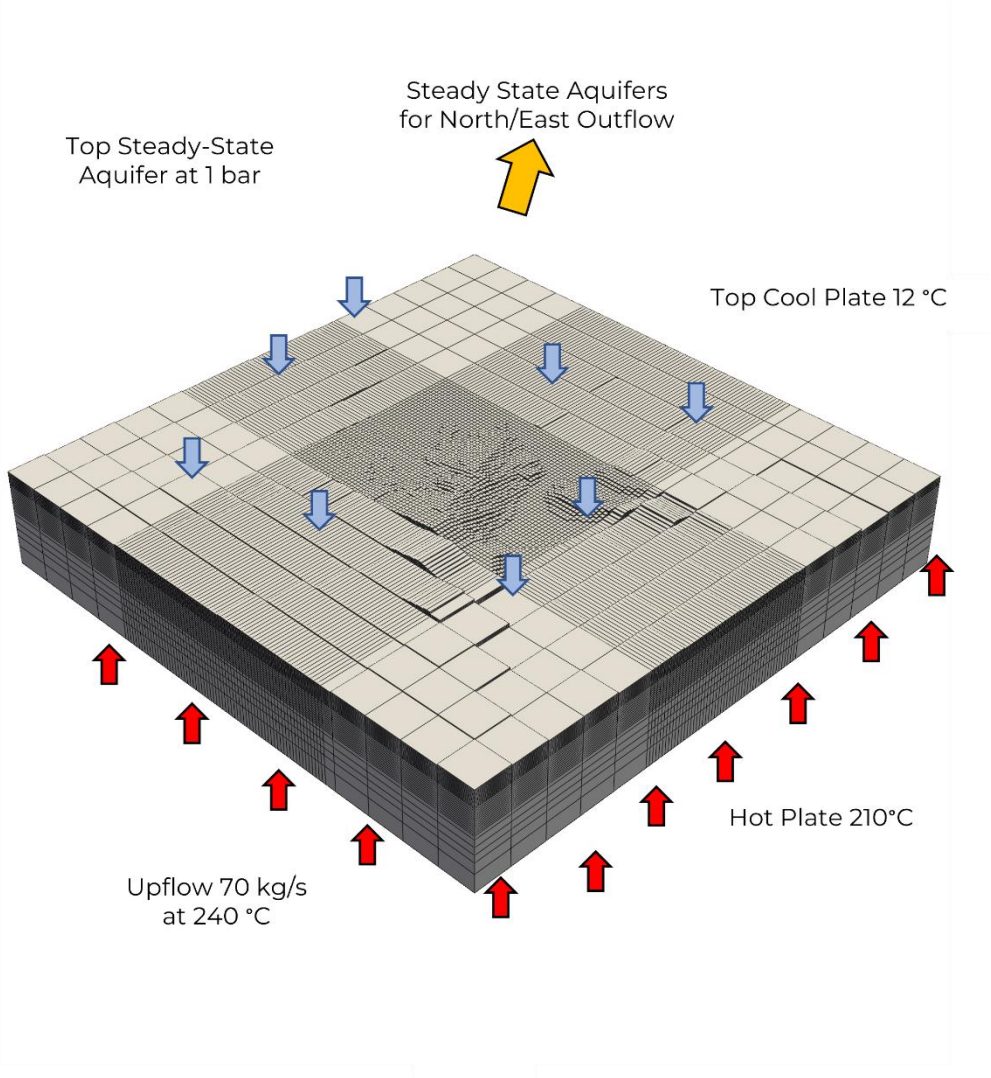

Figure 6: Steamboat Boundary Conditions Summary.

2.2 Natural State

The numerical model is simulated to natural state conditions for 100,000 years with the boundary conditions. Figure 7 shows the permeability structures that act as major fluid flow pathways across the reservoir.

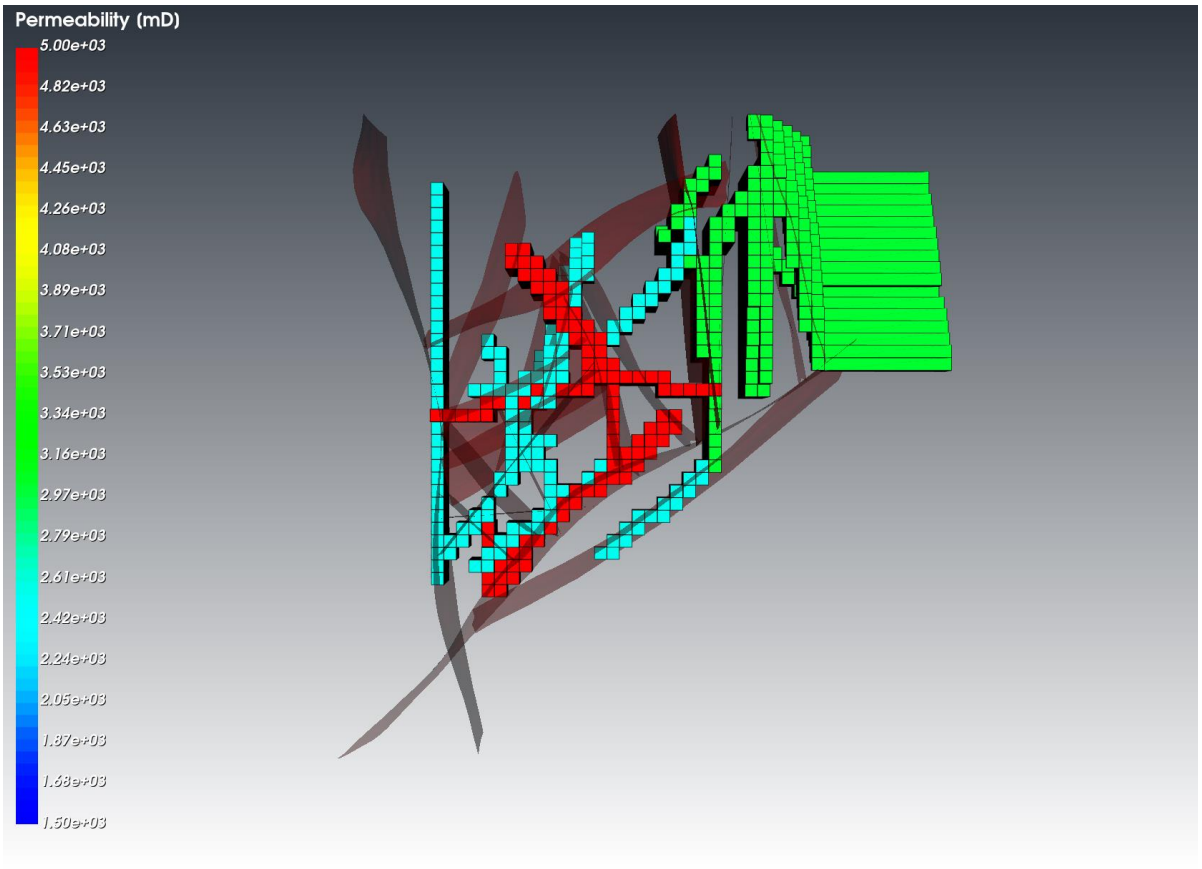

Figure 7: Reservoir model permeability structures based on the conceptual model. The upflow is below the major faults in Upper Steamboat (Southern part of the model). The high permeability faults act as fluid migration pathways from Upper Steamboat to Lower Steamboat and towards the outflow zone.

The natural state of the reservoir model is calibrated to stable static downhole pressure/temperature surveys from the field. Early temperature surveys are used to calibrate the natural state of the reservoir by selecting the most reliable data for different areas of the reservoir. The temperature match is particularly important at reservoir depths near the feed zones and the simulation results closely matches with the survey data. There are some wells that are not a perfect match in downhole temperature profiles, but the model is considered at natural state with a close match at feedzone depths. The pressure distribution also fits the measured and interpreted static pressure data. The simulated temperature and pressure are matched to the closest date of the measurement. The temperature distribution at Steamboat follows a deep upflow below Upper Steamboat and an outflow regime along the major structures. The hottest wells are at Upper Steamboat with temperature ranging between 215°C to 240°C, with a reversal seen at elevations ranging from 800-1000 mRSL The temperature decreases significantly at Middle Steamboat where the hottest wells are around 150°C to 190°C. The temperature distribution is more uniform towards Lower Steamboat with temperatures ranging from 160°C to 168 °C. The shallow depths of Lower Steamboat wells means that there is little reversal observed. The temperature distribution follows the permeability pathways in the reservoir, with the main faults acting as conduits for heat and mass transport in Upper and Middle Steamboat and a more distributed heat at Lower Steamboat. Figure 8 shows the interpreted natural state temperature at different areas of the field and pressure at Steamboat. Figure 9 shows the interpreted temperature distribution along the Upper, Middle and Lower Steamboat used for natural state model.

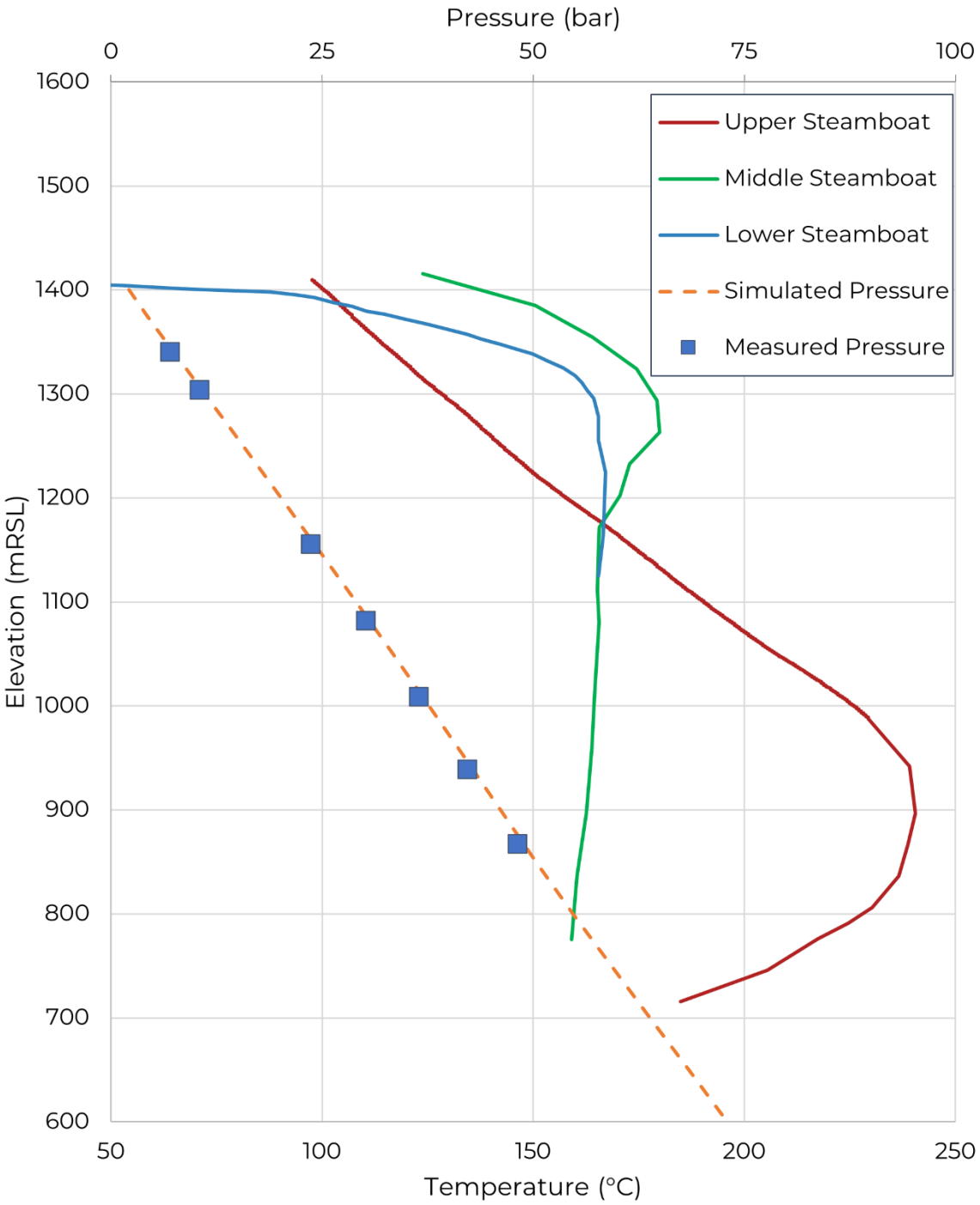

Figure 8: Natural state pressure and interpreted temperature distribution at Upper, Middle and Lower Steamboat. The measured pressure data is taken from all areas of the field which suggests that there is negligible horizontal pressure gradient. Reservoir model simulates the natural pressure by specifying a hydrostatic pressure boundary. Temperature distribution suggests that the deep permeability at Upper Steamboat rises significantly as it reaches Middle and Lower Steamboat.

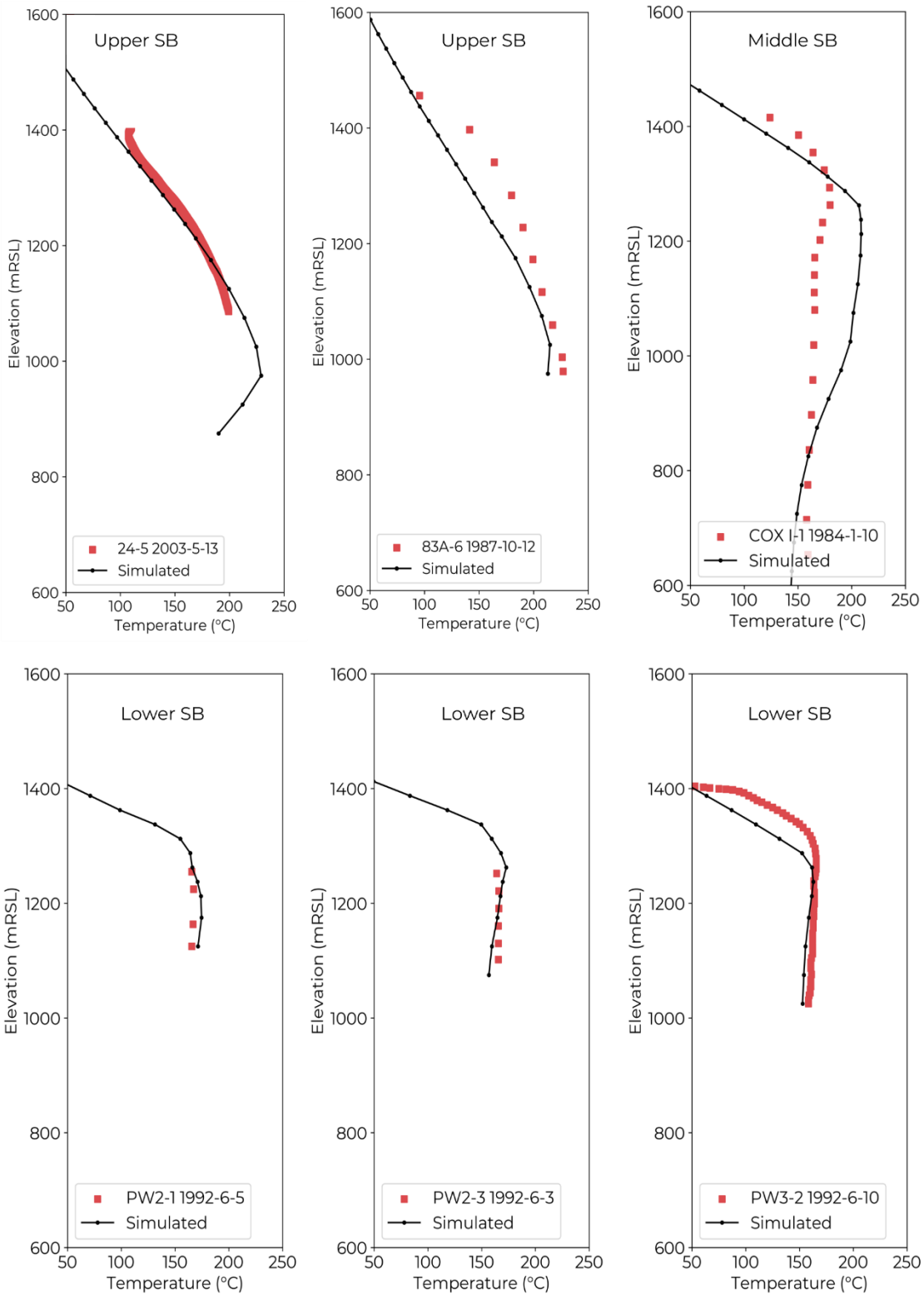

Figure 9: Natural state temperature distribution along wellbores.

2.3 Calibration

Well feedzones were estimated based on downhole pressure/temperature/spinner (PTS) surveys, drilling breaks and information collected during well tests, and correspond to major structures and fractured zones in the reservoir conceptual model and natural state. A robust data set for calibration is available based on historical and ongoing production at Steamboat. Wellfield data from before 2006 are sporadic

and injection rates were not always measured. Therefore a 90% reinjection of the fluid was assumed based on steam losses, due to evaporative cooling from a water-cooled cooling tower at Steamboat Hills until 2020.

2.3.1 Pressure Calibration

Historical development at Steamboat was dominated by shallow production wells at Lower Steamboat for direct use and recreation, and later flash steam generators with about 80-90% reinjection at Steamboat Hills steam generator and 100% reinjection at Steamboat 1,2 and 3 (Combs and Goranson, 1994). Sorey and Colvard (1992) attributed the changes in shallow ground water levels to an increase in water use in the Truckee Meadows and suggested monitoring pressure at deep geothermal wells. In the absence of continuous, long-term pressure monitoring, the numerical model was calibrated using short-term pressure change during outages (Figure 10) and recent pressure monitoring at shallow wells (Figure 11). Historically, pressure has remained consistent throughout the Steamboat geothermal field with only minor fluctuations, despite less than 100% reinjection earlier in the field's operation as seen in data from periodic static pressure surveys in Figure 12.

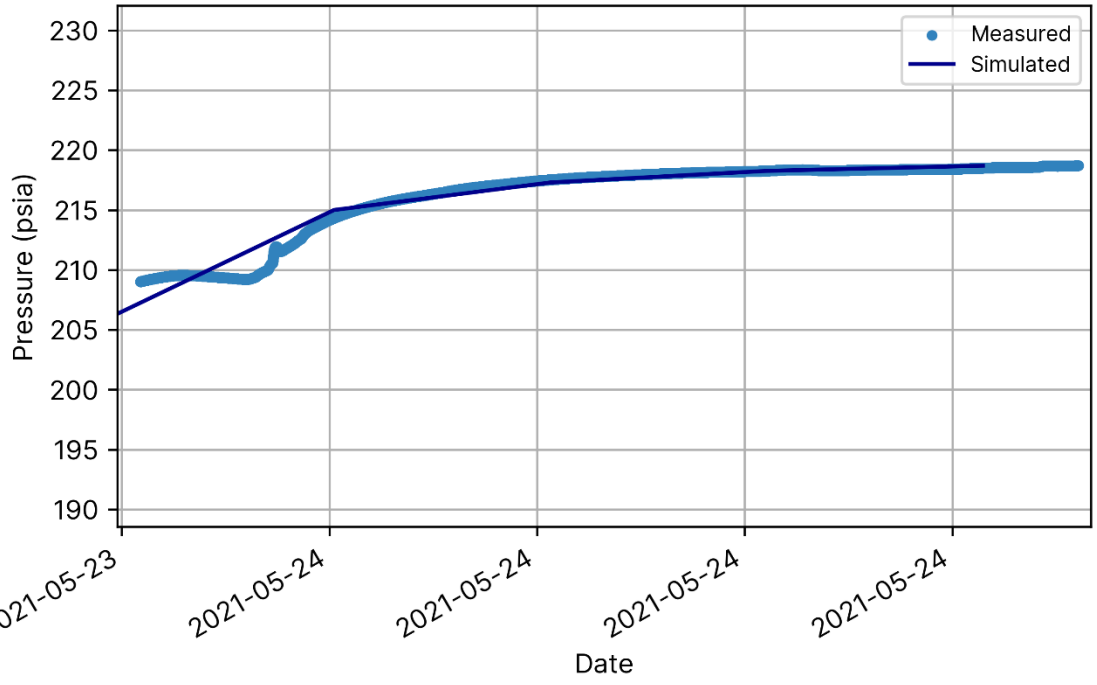

Figure 10: Steamboat 83-6BRD downhole pressure measurement during a planned partial plant outage in 2021.

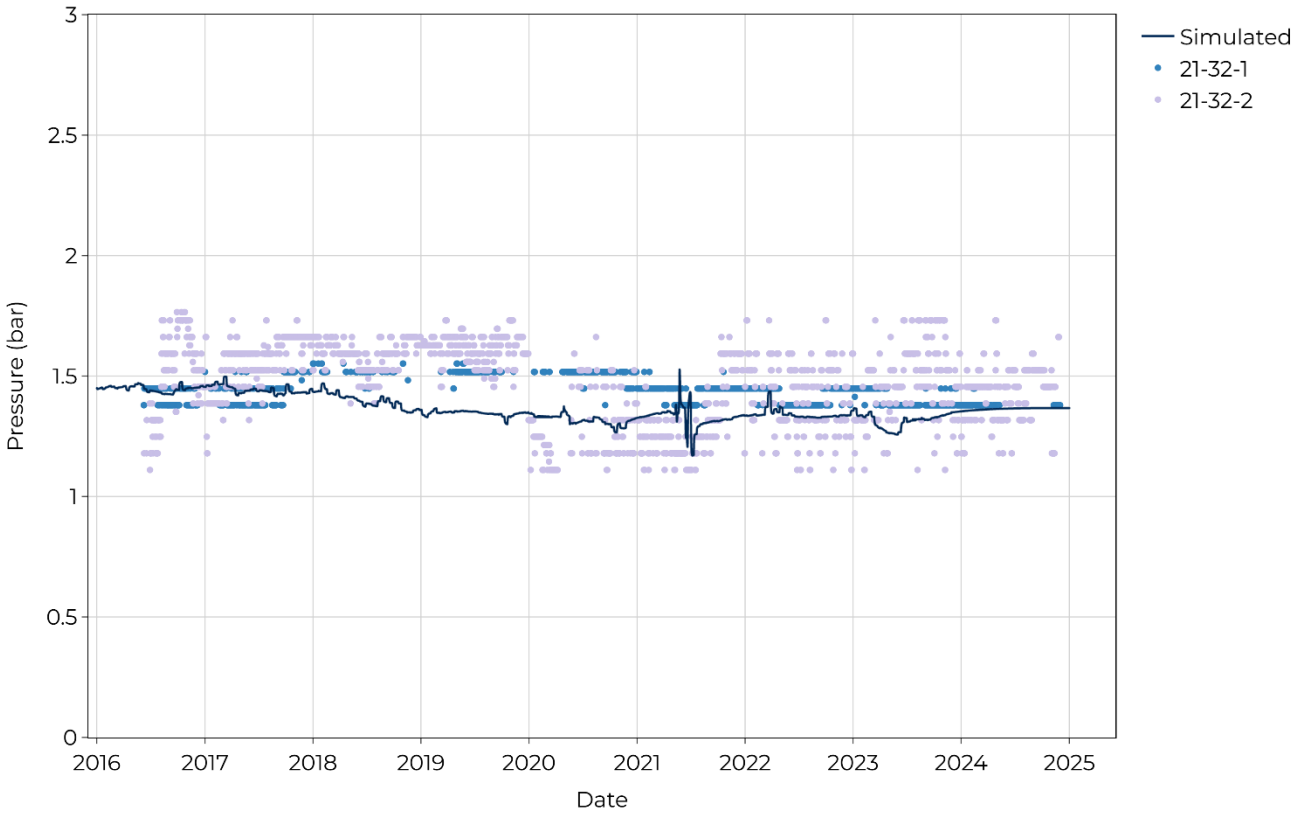

Figure 11: Steamboat 21-32 simulated pressure compared with shallow monitoring pressure.

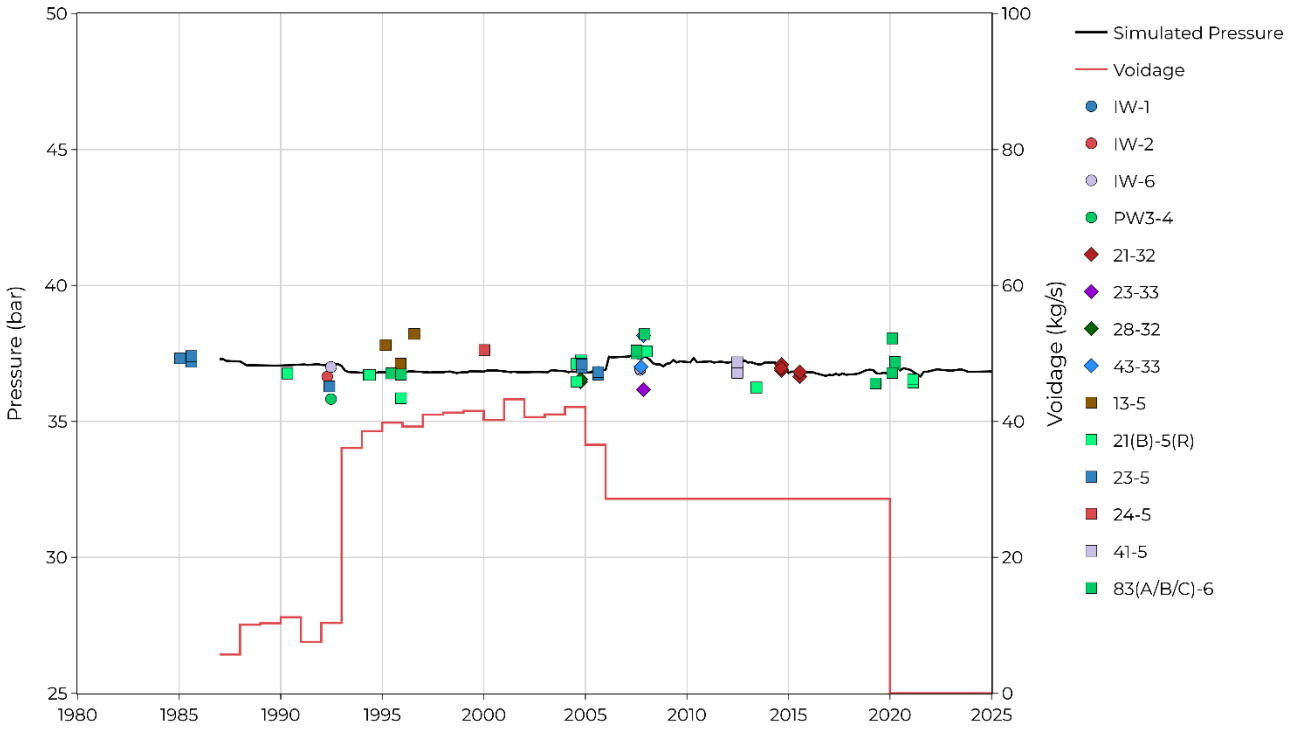

Figure 12: Downhole pressure interpolated at +1000 mRSL elevation at different locations at Steamboat using downhole survey data collected at various times throughout the operational history. Different shapes in plotted points indicate Lower, Middle and Upper Steamboat wells, which suggest there is uniformity in pressure data across the field. Simulated pressure changes with net annual average voidage (difference between production and injection rates).

2.3.2 Temperature Calibration

Temperature decline at individual producers and weighted average of the three areas of Steamboat are calibrated in the numerical model. An overall temperature decline from the simulation (1.8 °C/year since 1988 and 0.89 °C/year in the last 10 years) closely matches the measured data (1.86°C/year and 1.1 °C/year respectively). Middle Steamboat wells had been cooled prior to the start of production due to the proximity of injectors used to support production at Upper Steamboat. Figure 13 and Figure 14 show the temperature history at Steamboat. Temperature data prior to 2006 are sporadic and have been interpolated from sources such as Tracer Flow Test (TFT) data and Pressure-Temperature surveys.

All production wells are grouped into Upper Steamboat, Middle Steamboat, and Lower Steamboat wells for overall calibration of temperature declines. The wells are listed in Table 2.

Table 1: Steamboat Production Well classification.

Well Group	Wells
Upper Steamboat	13-5RD, 21-5, 21-5R, 21B-5R, 23-5, 24-5, 41-5, 83A-6, 83B-6RD, 83C-6
Middle Steamboat	14-33, 14A-33, 28-32, 34-32, 44-32, 44A-32
Lower Steamboat	78-29, HA-4, PW-1, PW-2, PW-3, PW2-1, PW2-3, PW2-5, PW3-1, PW3-2, PW3-3, PW3-4

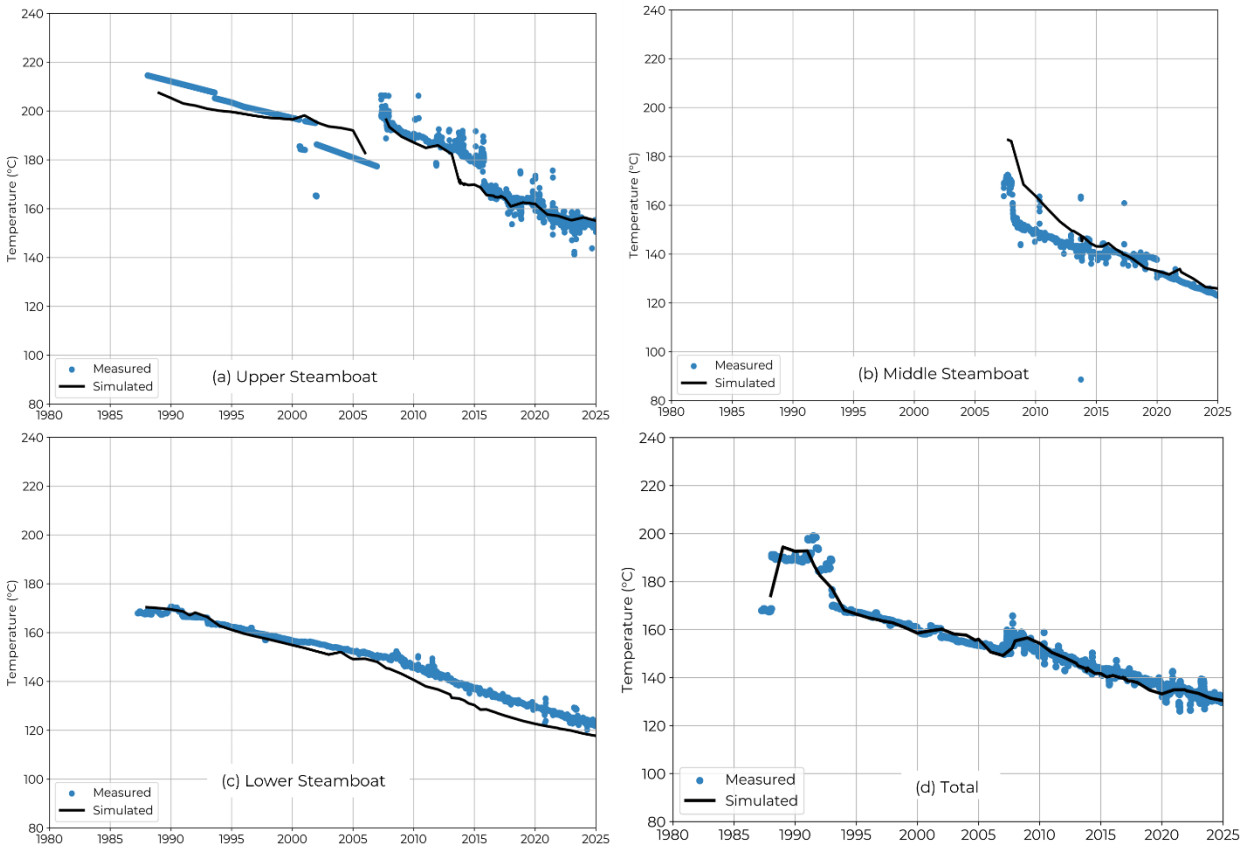

Figure 13: Weighted average temperature calibration at Steamboat (a). Upper Steamboat production wells, (b) Middle Steamboat production wells, (c) Lower Steamboat production wells and (d) Total field weighted average production.

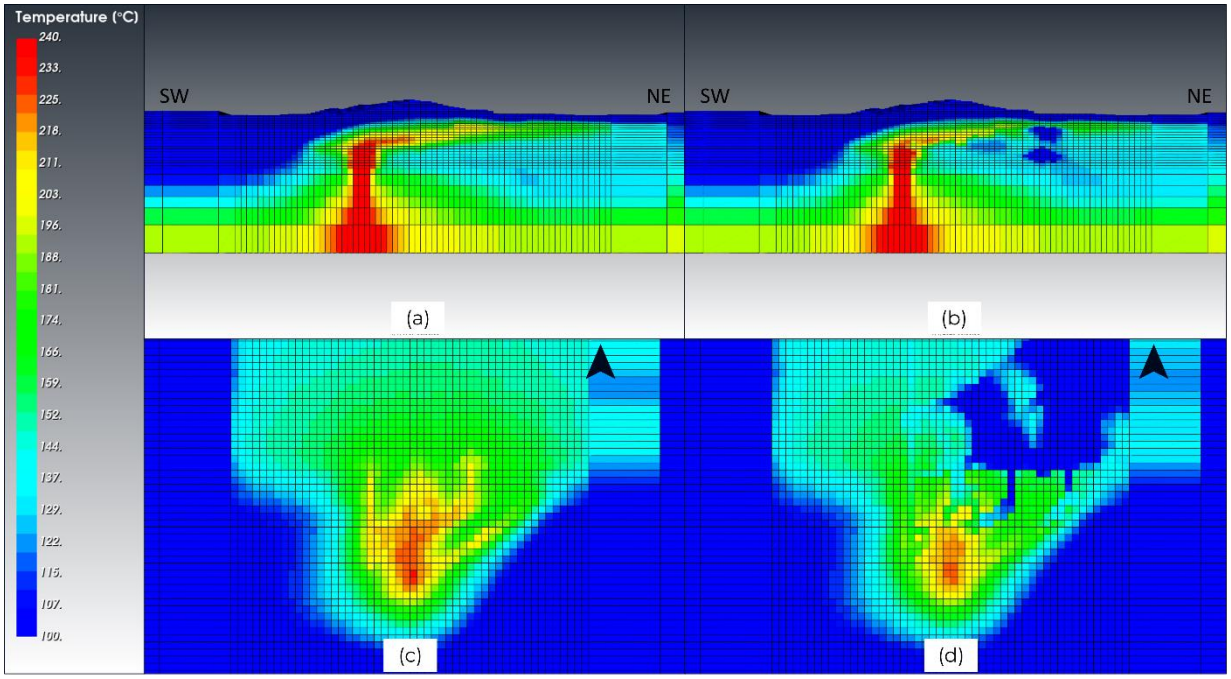

Figure 14: Temperature evolution at Steamboat (a). Temperature distribution in 1987 along Steamboat fault, (b) Temperature distribution in 2025 along Steamboat Fault, (c) Temperature distribution in 1987 at 1050 mRSL (d) Temperature distribution in 2025 at 1050 mRSL.

2.3.3 Tracer Calibration

Thermally stable tracers are used for identifying the preferential pathways for geothermal fluids. There have been five tracer studies done at Steamboat using a total of 14 injectors with an average tracer injection of 100 kg and 44 different measurement points (production and water wells). Based on the results, fluid flow pathways are identified and corroborated with structural interpretations. Despite the close spatial distribution of injectors at Lower Steamboat (IW-3, IW-5), the deeper injection feedzones and high background permeability cause low (less than 15 ppb) but fast tracer returns (before 30 days) (Figure 15). Tracer injection at Middle Steamboat wells (23-33, 21-32, 64A-32, and 43-33) were measured mostly at Lower Steamboat with low (less than 25 ppb) and slower tracer returns (up to 90 days), and very little tracer recovered at Upper Steamboat producers.

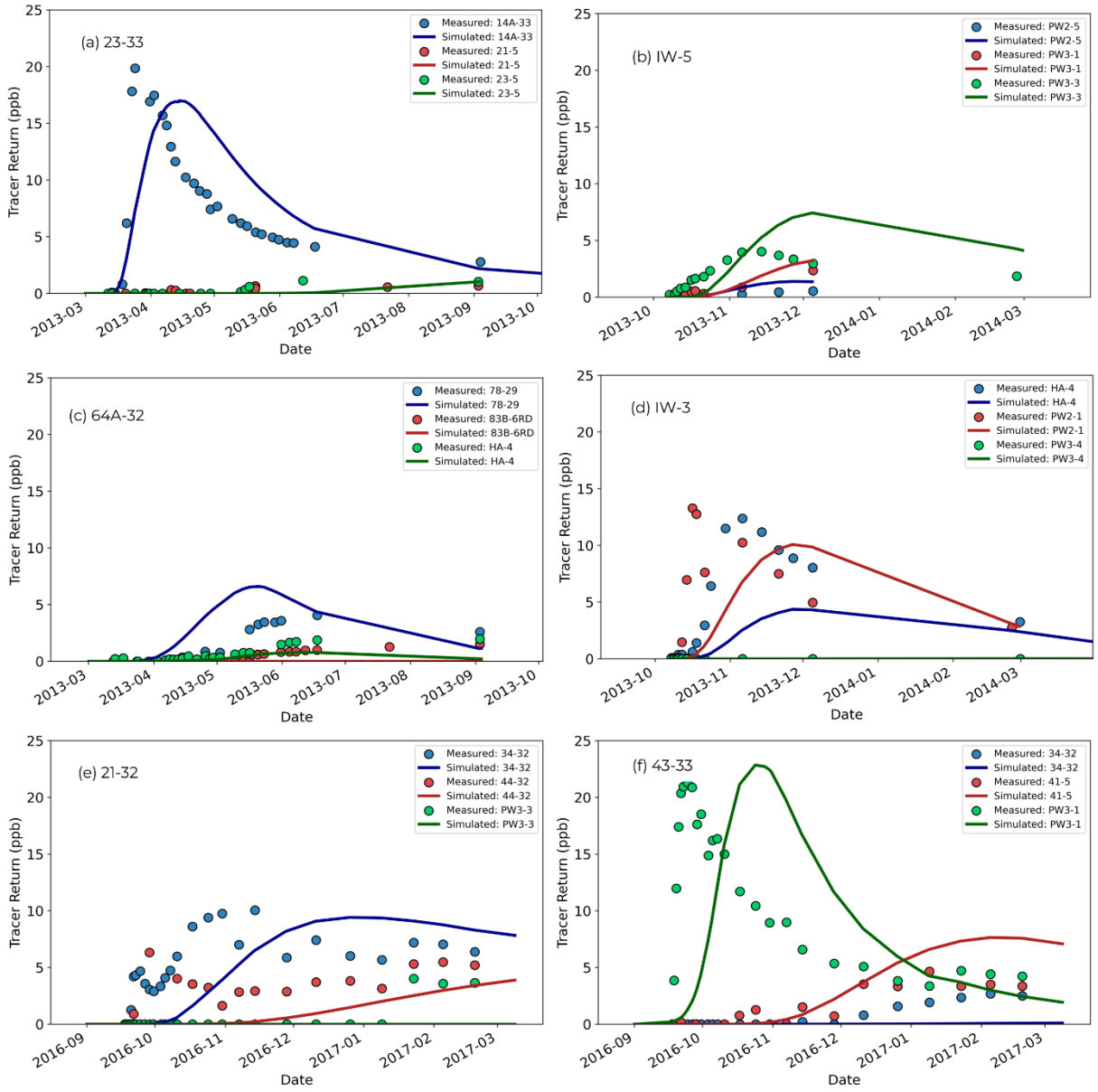

Figure 15: Tracer returns calibration from different tracer injection wells. (a) 23-33, (b) IW-5, (c) 64A-32, (d) IW-3, (e) 21-32, (f) 43-33.

CONCLUSION

The Steamboat geothermal field is a complex geothermal system that has had a long history of development. The presented numerical model is a significant update from previous modeling efforts. This model was guided by the updated conceptual model which combines the geoscience and reservoir engineering expertise at Ormat. The numerical model implementation of the structural model benefited from favoring simplicity where possible. The model uses an up-to-date wellfield history, the latest numerical modeling tools and incorporates

recently observed temperature trends. There are areas for future improvement in the model with some individual well calibrations. The model will be continuously improved and periodically updated to reflect wellfield changes and observations.

This case study of Steamboat numerical model is also being used to guide operational and reservoir management decisions at Steamboat and other Ormat fields for collaborative and consistent model updates. The proximity of the geothermal resource and power plants to a large population center in Reno is very advantageous for local power supply and grid stability, however, it does make it important to monitor and predict changes in ground water level associated with the geothermal resource. The pressure data collected at various times in the history of the field suggests that geothermal development in the area has not been a primary cause of any changes observed. By undertaking a repower of the Steamboat Hills plant with the Steamboat Hills Repower, which is a modern air-cooled binary plant, no mass loss is observed between the production and injection and therefore will continue to support reservoir pressure through time.

Acknowledgements

The authors thank Ormat Technologies, Inc. for permission to publish this work. We also appreciate Mauro Parini for his technical review of the model and his insight. Thanks to everyone who have been at Ormat in the past for their work on Steamboat, especially Chris Gates who led the development of the conceptual model.

REFERENCES

Ayling, B. F. (2020, February). 35 years of geothermal power generation in Nevada, USA: a review of field development, generation, and production histories. In 45th Workshop on Geothermal Reservoir Engineering, Stanford University, Stanford, California.

Bjornsson, G., Arnaldsson, A., Akerley, J., & Geothermal, R. (2014). A 3D numerical reservoir model for Steamboat, Nevada. Geothermal Resources Council Transaction, 38, 917-926.

Blackwell, D.D. (2013) The Thermal Structure of the Continental Crust. In Geophysical Monograph Series, edited by John G. Heacock, 169–84. Washington D. C.: American Geophysical Union.

Combs, Jim, and Colin Goranson. Use of slim holes for reservoir evaluation at the Steamboat Hills Geothermal Field, Nevada, USA. No. SGP-TR-147-19. Geo Hills Associates, Los Altos Hills, CA; Geological Engineering Consultant, Richmond, CA, (1994).

dePolo, C. M. (2017). The Washoe Shear Zone Transtensional Hypothesis, A Reconnaissance Study.

Feucht, D., Gates, C., Selwood, R., Churchill, M., Zuza, R. (2023). Magnetotelluric Data Acquisition in a High-Noise Environment: Results from the Steamboat Hills Geothermal Complex, Nevada, USA. Geothermal Resources Council Transactions, 47, 1895-1914.

Franz, P., & Clearwater, J. (2021). Volsung: A Comprehensive Software Package for Geothermal Reservoir Simulations. In Proceedings of World Geothermal Congress.

Goranson, C., van de Kamp, P., & DeLong, T. (1990). Geothermal Injection and Monitoring Program History at the Caithness Power Inc. Flash Steam Power Plant Steamboat Springs, Nevada. In Proceedings of the Symposium on Subsurface Injection of Geothermal Fluids, Oct. 29 (Vol. 30, pp. 101-123).

Kennedy, B. M., & Van Soest, M. C. (2007). Flow of mantle fluids through the ductile lower crust: helium isotope trends. Science, 318(5855), 1433-1436.

Putirka, Keith, Marlon Jean, Brian Cousens, Rohit Sharma, Gerardo Torrez, and Chad Carlson. (2012). Cenozoic Volcanism in the Sierra Nevada and Walker Lane, California, and a New Model for Lithosphere Degradation. Geosphere 8, no. 2: 265–91.

Richardson, I., & Webbison, S. (2024). Greenhouse Gas Emissions Reduction: Global Geothermal Power Plant Catalog. GRC Transactions, 48.

Silberman, M. L., White, D. E., Keith, T. E., & Dockter, R. D. (1979). Duration of hydrothermal activity at Steamboat Springs, Nevada, from ages of spatially associated volcanic rocks (No. USGS-PP-458-D). Geological Survey, Washington, DC (USA).

Sorey, M. L., & Colvard, E. M. (1992). Factors affecting the decline in hot-spring activity in the Steamboat Springs area of critical environmental concern, Washoe County, Nevada. US Geological Survey Administrative Report for the Bureau of Land Management.

Sorey, M., & Spielman, P. (2017). Rates of thermal water discharge from the hot water geothermal system beneath the Steamboat Hills in Western Nevada, USA. Geothermics, 69, 202-206.

Wagner, W., & Kretzschmar, H. J. (2008). IAPWS industrial formulation 1997 for the thermodynamic properties of water and steam. International steam tables: properties of water and steam based on the industrial formulation IAPWS-IF97, 7-150.

Walsh, P., Martini, B. A., & Spielman, P. (2010). High angle fracture-controlled permeability at upper Steamboat Hills geothermal field, NV. Geothermal Resources Council Transactions, 34, 833-837.

White, D. E. (1967). Some principles of geyser activity, mainly from Steamboat Springs, Nevada. American Journal of Science, 265(8), 641-684.

Wisian, K.W., Blackwell, D.D., and Richards, M. (1999). Heat Flow in the Western United States and Extensional Geothermal Systems. Twenty-Fourth Workshop on Geothermal Reservoir Engineering, 8 p. Stanford, California.